Proc. Natl. Acad. Sci. USA
Vol. 90, pp. 2212–2216, March 1993
Neurobiology

Dynamic and distributed properties of many-neuron ensembles in the ventral posterior medial thalamus of awake rats

(multi single-unit recordings/somatosensory system/receptive field/population responses/neuronal networks)

MIGUEL A. L. NICOLELIS*†‡, RICK C. S. LIN*, DONALD J. WOODWARD§, AND JOHN K. CHAPIN*

*Department of Physiology and Biophysics, Hahnemann University, Philadelphia, PA 19102-1192; †Department of Pathology, University of Sao Paulo, Sao Paulo, Brazil CEP 01246; and, §Department of Physiology and Pharmacology, Wake Forest University, Winston-Salem, NC 27109

Communicated by Irving T. Diamond, November 23, 1992

ABSTRACT **The traditional view that the map of the face in the ventral posterior medial thalamus (VPM) is static and highly discrete was derived largely from qualitative studies that reported only small, robust, and nonoverlapping receptive fields (RFs). Here, by using more quantitative techniques, we have provided evidence for an alternative hypothesis: the RFs in the VPM are large and overlapping and tend to shift as a function of post-stimulus time. These results were obtained through simultaneous recordings of up to 23 single neurons across the whisker representation in the VPM of rats. Under both awake and anesthetized conditions, these neurons responded robustly at short (4–6 ms) and/or long (15–25 ms) latencies to discrete vibromechanical stimulation of single facial whiskers. Computer graphics were used to construct three-dimensional plots depicting the magnitudes of neuronal responses to stimulation of each of several whiskers as a function of post-stimulus time. These "spatiotemporal RFs" demonstrated that (*i*) the RFs of VPM neurons are quite large, covering up to 20 whiskers and (*ii*) the spatial locations of these RFs may shift dramatically over the first 35 ms of post-stimulus time, especially from the caudal-most to the rostral-most whiskers on the face. These results suggest that the VPM contains a dynamic and distributed representation of the face, in which stimulus information is coded in both spatial and temporal domains.**

As an organizing principle, the sensory systems of the mammalian brain have long been considered to be built around an ascending series of highly secure, static, and topographic representations of the receptor surface. In particular, neurons within the dorsal column lemnisco–thalamic pathway, including the primary somatosensory cortex (SI), have classically been thought to securely preserve the spatial, temporal, and submodal characteristics of cutaneous receptors (1–3).

In recent years, this doctrine has been challenged by demonstrations that the SI cortical sensory map can be changed by certain manipulations, such as peripheral deafferentation (4) or repetitive tactile stimulation (5). Furthermore, sensory responses in the SI are modifiable by behavior (6, 7). Such results argue that, as opposed to the traditional static and local (nonoverlapping) model, the SI map may be more dynamic (i.e., changing as a function of time) and distributed (i.e., overlapping). Despite these advances in our conceptualization of the SI, subcortical structures, such as the rat ventral posterior medial thalamus (VPM), are still generally considered to contain highly static and spatially specific representations of the periphery (8–10). This is surprising in view of the well-known anatomical convergence of feed-forward and feed-back influences on this thalamic nucleus (11–16). This convergence could provide a substrate for dynamic and distributed information processing in the VPM.

The original theory of the static discrete thalamic map was based largely on qualitative studies using deeply anesthetized animals (3, 8–10). For example, receptive fields (RFs) in the rat VPM were reported to cover only a single whisker (8–10). In contrast, larger RFs (four to six whiskers) have been reported by studies that utilized post-stimulus time histograms (PSTHs) to measure neuronal sensory responses to whisker stimulation (17–19).

To date, however, no study has utilized statistically verified quantitative measurements to measure the full spatial extent of RFs in the awake rat VPM or to show how these RFs change as a function of post-stimulus latency. The accurate measurements of RFs here required several technological advances. First, techniques were developed allowing chronic recording and simultaneous discrimination of large numbers of single neurons (up to 23 per animal) across the sensory representation of the face in the VPM in awake or anesthetized rats. Unlike traditional techniques in which single units are recorded in serial order, our approach allows the RFs of large numbers of neurons to be characterized concurrently. Not only does this circumvent the nonstationarity problems of serial unit recording, but also it dramatically increases the data yield. This allowed implementation of our highly quantitative procedures, which require 4–6 h to characterize an RF.

Our results demonstrate that RFs in the rat VPM are larger than previously reported and also exhibit complex spatiotemporal properties, suggesting that this nucleus contains a dynamic and distributed sensory representation.

METHODS

Chronic simultaneous recordings of the extracellular activity of up to 23 single neurons per animal were obtained through arrays of microwire electrodes. Eight to 16 25–50 μm Teflon-coated stainless steel microwires (NB Labs, Denison, TX) were first implanted across the ventral posterior thalamus of 10 adult Long–Evans (hooded) rats (250–300 g) under pentobarbital (50 mg/kg, i.p.) anesthesia. The final position of the wire bundle was verified by monitoring the RFs of unit clusters recorded from the microwires during the implant surgery. After 1 week, rats were placed in the experimental apparatus and signals from all of the microwires were simultaneously recorded using a 64-channel amplifier-filter-discriminator system, obtained from Spectrum Scientific (Dallas). This employed digital signal processors to perform time–voltage discrimination (using three windows) of digi-

The publication costs of this article were defrayed in part by page charge payment. This article must therefore be hereby marked "*advertisement*" in accordance with 18 U.S.C. §1734 solely to indicate this fact.

Abbreviations: PSTH, post-stimulus time histogram; RF, receptive field; SI, primary somatosensory cortex; VPM, ventral posterior medial thalamus; 3D, three-dimensional.

‡To whom correspondence and reprint requests should be addressed at: Department of Physiology and Biophysics, Mail Stop 409, Hahnemann University, Broad and Vine Streets, Philadelphia, PA 19102-1192.

tized (40 kHz) waveforms obtained from each microwire. The discrimination was validated on-line by plotting each sample waveform as a dot (as in Fig. 1*A*) within an x–y space defined by components 1 and 2 of a principal components analysis of typical spike waveforms (20, 21).

Recordings were obtained in both awake and pentobarbital-anesthetized conditions. Since more than one discriminable single unit could often be recorded from each microwire, 8–23 single units were routinely recorded per animal in each experiment (Fig. 1*B*). PSTHs were constructed by plotting the time of each recorded spike in relation to the onset times of computer-controlled deflections of each of 7–20 whiskers using a vibromechanical stimulus probe. Stimuli consisted of 0.5-mm step displacements of 100-ms duration delivered at 1 Hz. Large whiskers were deflected ≈3°, in an initially up direction. Stimulation of single whiskers in awake freely moving rats was made possible by using animals highly habituated to human handling. Typically 250–500 consecutive stimulation trials were obtained for each whisker. Computer analysis of the PSTHs allowed measurement of the magnitudes of short- and long-latency responses to these stimuli. For this, the PSTHs were divided into seven post-stimulus epochs: 3–5, 5–10, 10–15, 15–20, 20–25, 25–35, and 35–50 ms. The response magnitude during each epoch was expressed in instantaneous frequency of firing (in spikes per s; i.e., Hz). The statistical significance of each of these sensory-evoked responses was tested by using both a Kolmogorov–Smirnov test and also analysis of variance with a Dunnet's post-hoc test (significance level: $P < 0.01$). Spatial distributions of sensory responses in each epoch were compared using a χ^2 test. Latencies of sensory responses were determined by locating inflection points in post-stimulus cumulative frequency histograms. Spatiotemporal neuronal RFs were depicted by color-coded three-dimensional (3D) surfaces in which the magnitudes of each sensory-evoked response of a neuron were plotted as a function of stimulation site and post-stimulus time. These data were fitted to the surface through use of a spline algorithm based on a moving third-degree polynomial function.

RESULTS

A total of 132 neurons distributed across the ventral posterior thalamus was chronically recorded. Of these, 120 had cutaneous RFs on the face. All recording sites were confirmed histologically. By using the quantitative techniques described above, much larger and more dynamic RFs were observed in both awake and anesthetized preparations. Fig. 1*C* shows the spatial distribution of responses of a single thalamic neuron 5–10 ms after the independent stimulation of 20 whiskers during light pentobarbital anesthesia. Responses were plotted in a 3D grid representing the rat whisker pad. Although

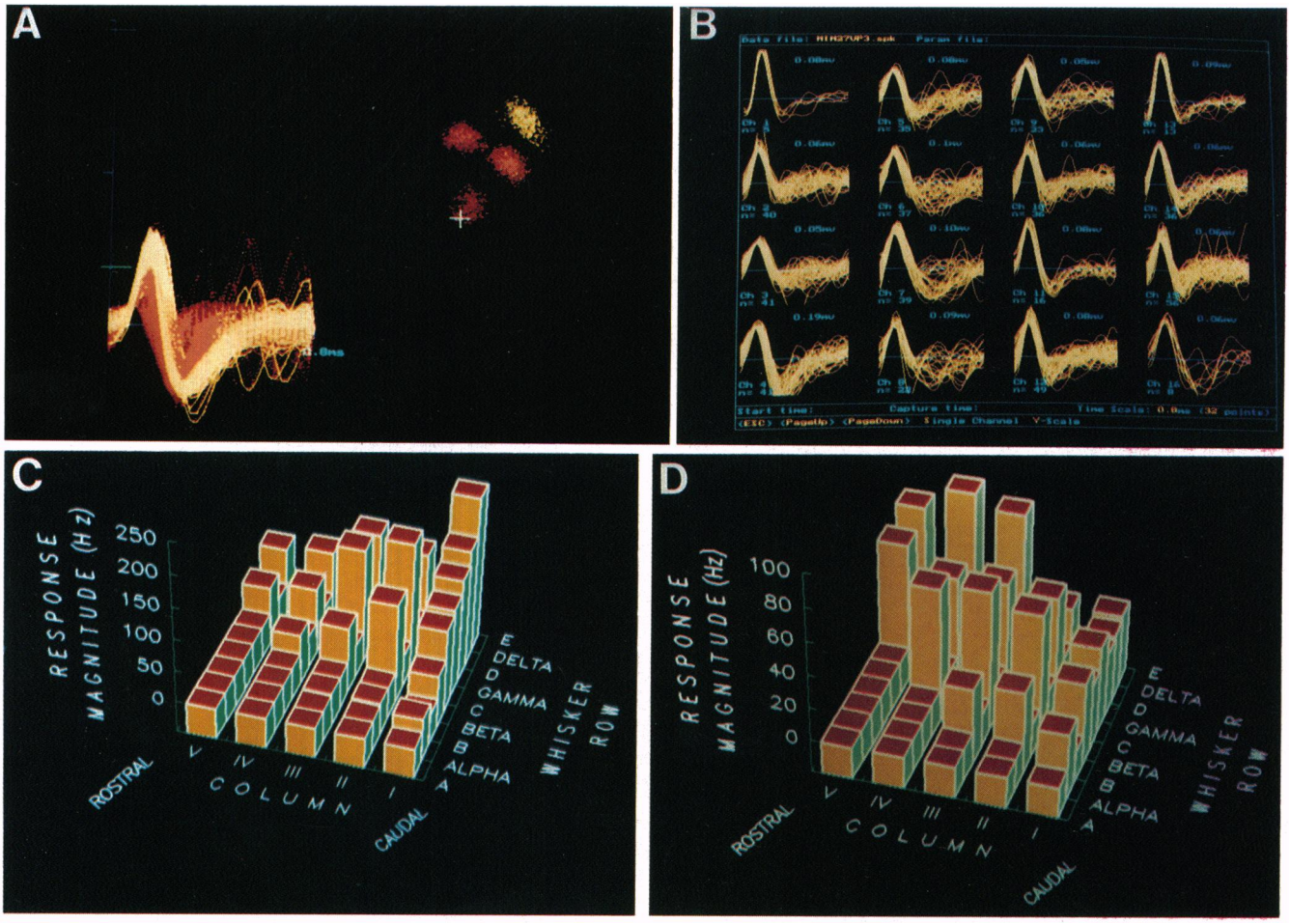

FIG. 1. (*A*) Multiple spike waveforms from a single electrode were classified by plotting them within a two-dimensional space defined by principal components analysis (see text). For this discrimination, both accepted (yellow) and rejected (red) waveforms (left) were plotted as dots in the cluster diagram (right). The yellow cluster shows successful discrimination of one single unit from three other single unit clusters (red). (*B*) Superimposed digitized waveforms of 16 single VPM neurons simultaneously recorded in an awake rat. (*C* and *D*) Vertical bars in these 3D diagrams depict the magnitudes of response (in Hz: average instantaneous spikes per s) of a VPM neuron to stimulation of each of 20 whiskers arrayed on the face in columns (I–V) and rows (A–E, interspersed with alpha–delta). The center of response shifted from the caudal whiskers during the 5- to 10-ms post-stimulus time epoch (*C*) to the rostral whiskers by the 25- to 35-ms post-stimulus epoch (*D*).

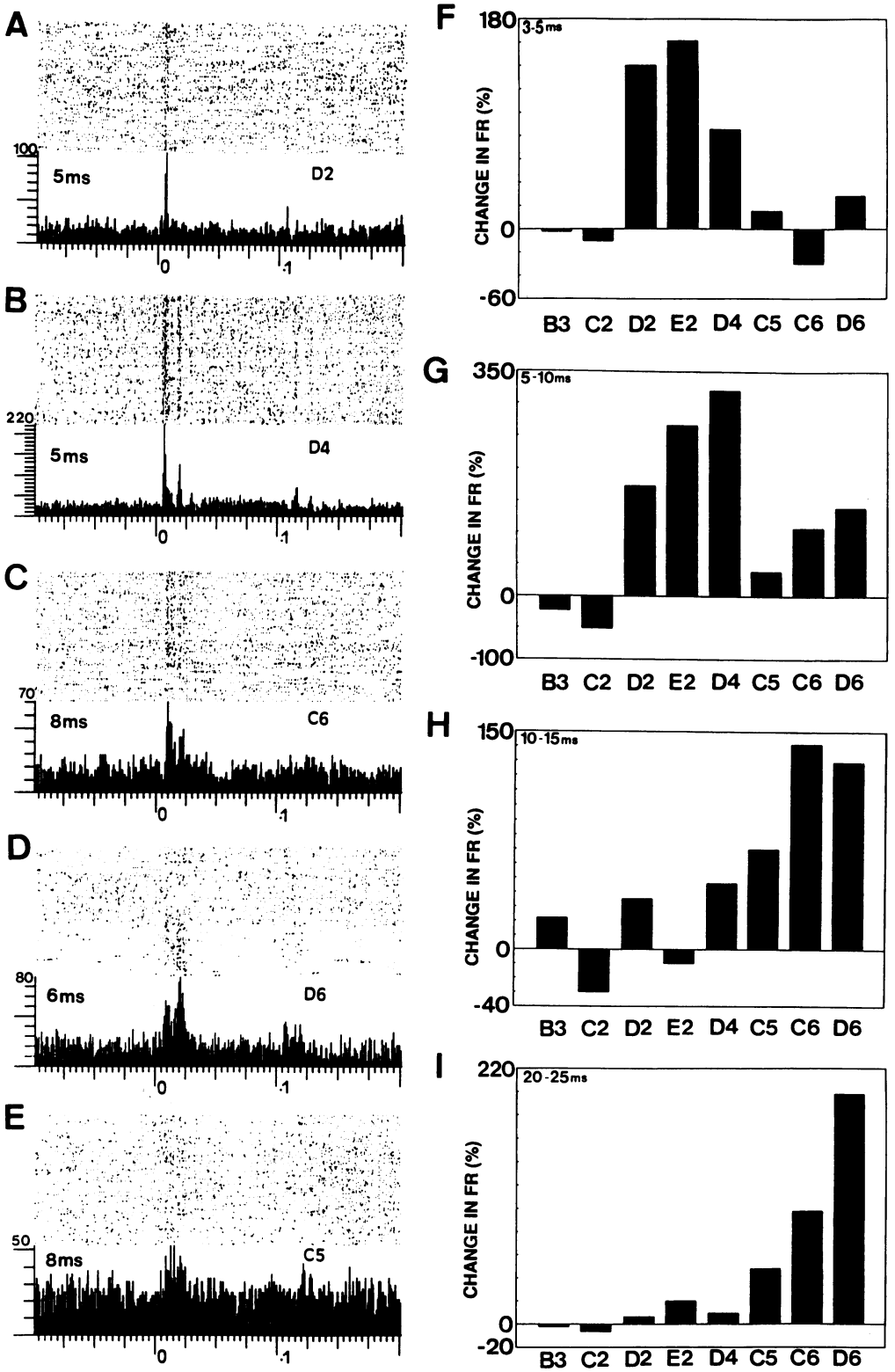

FIG. 2. (*A–E*) Raster plots and PSTHs show the responses of a single VPM cell to the independent stimulation of whiskers D2, D4, C6, D6, and C5, respectively, in an awake rat. Vertical axes are magnitudes of sensory response in Hz (small ticks = 10 Hz). Horizontal axes are time before and after whisker stimulation at 0 ms (small ticks = 5 ms). PSTH bins are 1 ms. Initial response latencies (in ms) are shown at left of each PSTH. (*F–I*) Bar graphs depict the caudal-to-rostral shift of RF centers over post-stimulus time. Ordinates show the magnitudes of this neuron's response (in percent increase or decrease over baseline firing) to stimulation of each whisker (labeled on abscissa) during four post-stimulus response epochs (indicated at top left of each frame).

the RF center of this cell was located in the caudal part of row E (response magnitudes ranging from 100 to 200 Hz), statistically significant responses were also obtained from stimulation of whiskers located across the E row and other rows.

All of the whisker-responsive VPM cells in this sample exhibited longer-latency excitatory responses (15–50 ms) to peripheral stimulation. When the spatial distributions of these later responses were characterized, they were often

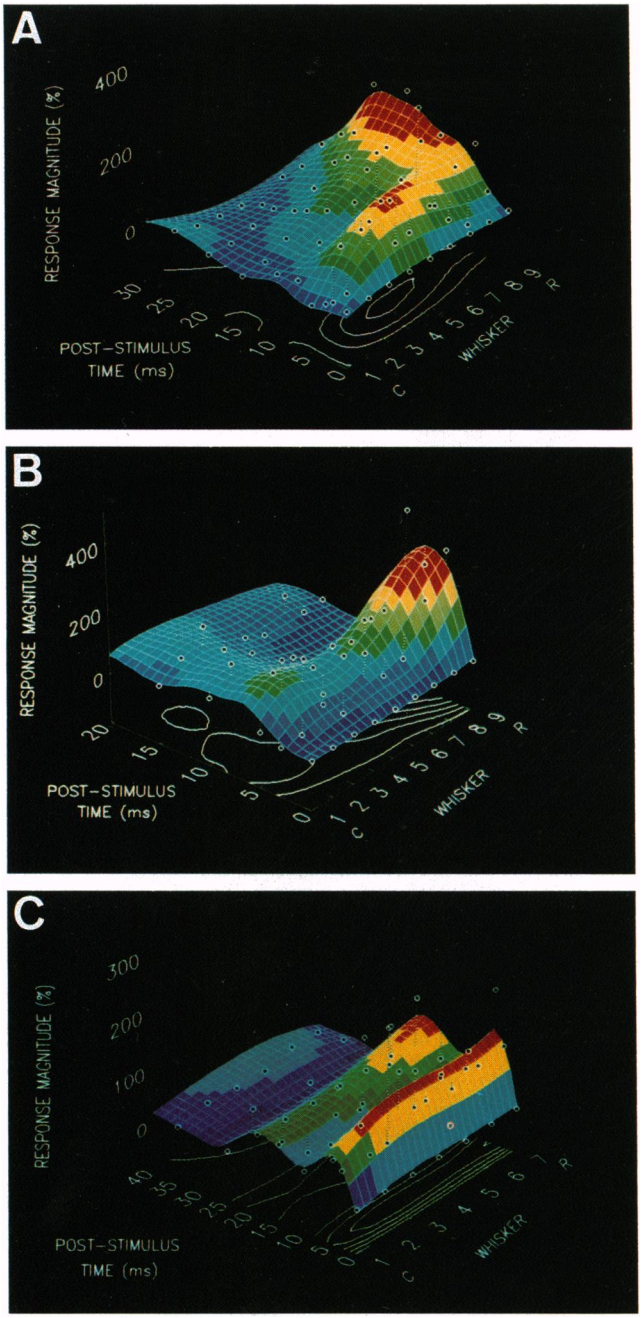

FIG. 3. Spatiotemporal RFs of three single neurons recorded in awake rats. These 3D diagrams show how RFs change across the spatial and temporal domains by graphing the magnitude of sensory responses (vertical axis) as a function of the whisker stimulated (right horizontal axis) and as a function of the post-stimulus time epoch (left horizontal axis). Stimulated whiskers were rank-ordered according to their relative caudal (C)-to-rostral (R) position. Neuronal response magnitudes were expressed as percent increased (or decreased) firing rates (FRs) during the indicated post-stimulus response epoch over the background FR. The white open circles over the surfaces show the FRs calculated from PSTHs for each post-stimulus epoch before the spline smoothing. For each figure, the total range of response magnitude is scaled into six color coded levels, from indigo (negative values; i.e., inhibition) to red (highest positive values; i.e., RF centers). (*A* and *B*) Whisker sequence (1–9): B3, C2, D2, E2, C4, D4, C5, C6, and D6, respectively. (*C*) Whisker sequence (1–7): α, C2, D2, E2, E3, D4, and D5, respectively.

found to have changed markedly from the RF obtained at short latency. To illustrate, Fig. 1*D* shows the spatial distribution of sensory responses in the 25 to 35-ms epoch for the cell whose short-latency (5–10 ms) responses are shown in Fig. 1*C*. Therefore, over the 20-ms period after the initial response of this cell, its RF center shifted from the caudal whiskers of the E row to the rostral-most whiskers of the E row. The response distributions in Fig. 1 *C* vs. *D* were shown to be significantly different using a χ^2 test ($\chi^2 = 806.26$; df = 19; $P < 10^{-6}$).

Since anesthesia is known to alter the physiology of somatosensory neurons (22, 23), similar experiments were carried out in awake rats. Fig. 2 contains raster plots and PSTHs showing sensory-evoked responses of a single VPM neuron to controlled deflection of different single whiskers in an awake rat. This cell responded mainly to stimulation of the caudo–medial whiskers of rows D and E at short latency (e.g., D2, E2, and D4). During subsequent post-stimulus intervals, however, the RF center shifted progressively to rostral whiskers in rows C and D (e.g., C5, C6, and D6). Fig. 2 *F–I* graphically depict this cell's response to each of these seven whiskers over four post-stimulus time epochs (from 3 to 25 ms). This sequence of graphs demonstrates a continuous time-dependent caudal-to-rostral shift in the RF of this cell. All of the response distributions shown in Fig. 2 *F–I* were shown (by χ^2) to be significantly different ($P < 10^{-6}$), except for the pair represented in Fig. 2 *H* and *I*.

Virtually all (90–100%) of VPM neurons with short-latency RFs centered in the caudal whiskers were found to exhibit this type of caudal-to-rostral shift in their RFs. To visualize such shifts, we have used 3D computer graphics to construct "spatiotemporal RFs" (Fig. 3). These depict variations in the sensory responses of single neurons across post-stimulus time and across the stimulated whiskers. Fig. 3*A* displays a frequently observed type of spatiotemporal RF: At short latency (5–10 ms), a large RF was defined with predominant responses (ranging in magnitude from 45 to 110 Hz) located in caudal whiskers. Over the next 10–15 ms, the greatest responses (35–62 Hz) were observed after stimulation of the rostral whiskers.

Such time-dependent spatial shifts were much less frequent among neurons with short-latency RFs centered on the rostral whiskers. About 10–20%, however, exhibited weak rostral-to-caudal RF shifts. For illustration, the spatiotemporal RF in Fig. 3*B* shows a weak (9–24 Hz) short-latency response to the stimulation of rostral whiskers. Over 10–20 ms after stimulus, the RF center shifted to a small region of the caudal whisker pad (whiskers B3 and C2). Fig. 3*C* shows a third type of spatiotemporal RF shift in which the short-latency RF was larger than the longer-latency RF. Here, almost every whisker produced a significant short-latency response, but longer-latency (15–20 ms) responses were seen only after stimulation of the rostral-most whiskers (such as D5).

Finally, analyses of the "population responses" of simultaneously recorded ensembles of VPM neurons indicated that (*i*) for each given stimulus the same thalamic network produces a unique population response; (*ii*) a given population response comprises at least some weighted contribution from most of the individual elements of the network, defining a distributed representation; and (*iii*) population RFs also display complex spatiotemporal behaviors, defining a dynamic map.

DISCUSSION

These results suggest, first, that the sensory representation in the rat VPM may be much more coarsely coded (i.e., distributed), with large overlapping neuronal RFs than previously reported. Furthermore, as many of these RFs exhibit spatial shifts over the 20 ms after the initial responses, the VPM appears to contain a map of the cutaneous periphery that embeds both spatial and temporal components of sensory experience.

Overall, this spatiotemporal complexity may reflect a greater degree of functional afferent convergence on thalamic neurons than has previously been considered. Furthermore, it suggests the existence of a spatiotemporal coding in the VPM, which may bias some neurons to respond differentially to particular sequences of peripheral stimulation of the face. For example, the commonly observed shifting of RF centers from the caudal to the rostral whiskers may inscribe a directional preference of these neurons. It is interesting that the time frame (≈20 ms) of this spatial shift is consistent with the sweep times of whisker movements used by rats during vibrissal exploration of external objects (24). Furthermore, the caudal-to-rostral movements of the long caudal whiskers during such behavior (24) may relate to the caudal-to-rostral shifting of thalamic RFs observed here. Carvell and Simons (24) have suggested that the long caudal whiskers may be more important for recognition of objects in space, whereas the short rostral whiskers may be used only to locate these objects' position. Such a differential functional role for caudal and rostral whiskers is consistent with our findings that cells with short-latency RFs centered in caudal whiskers show much greater spatiotemporal shifting than do cells with short-latency RFs centered on rostral whiskers.

Although the neuroanatomical basis for the complexity of these RFs is not known, it could be attributed to the extensive spread of the dendritic trees of VPM neurons (10, 25). This should allow individual neurons to receive input from each of the multiple afferent systems that converge asynchronously on this nucleus (11–15). Differences in latency, magnitude, and temporal decay observed in the primary excitatory responses of VPM cells (Fig. 2) could be produced by the convergence of distinct trigeminothalamic pathways (10) on both proximal and distal dendrites of VPM neurons (26). Long-latency excitatory responses (15–25 ms) could be shaped by a combination of slow-ascending trigeminothalamic afferents (27) and feedback projections from the SI cortex (15, 28). On the other hand, the inhibitory responses seen in Figs. 2 and 3, which contribute to the shifting of the RFs, may be derived from the reticular thalamic nucleus (16).

Previously, Stevens and Gerstein (29) have demonstrated that cells in the cat lateral geniculate nucleus of the thalamus exhibit complex visual RFs that include spatially heterogeneous distributions of responses at different latencies. The fact that these results in the lateral geniculate nucleus are similar to ours in the VPM suggests that such dynamic and distributed sensory representations may be a general rule for organization of the mammalian sensory thalamus.

Heretofore, the concept of distributed network processing has been proposed only for the cortical level. For example, large populations of neurons in the motor cortex have been shown to jointly code for the direction of intended limb movements (30). Similarly, distributed networks of cells in the inferior temporal cortex have been reported to code for faces (31). Such a strategy could be used by neuronal networks in the somatosensory cortex. Our results further advance this notion by suggesting that thalamic networks, and perhaps networks from other subcortical structures, may actively contribute to the dynamics of distributed somatosensory representations in the cortex. This contribution from subcortical structures could be importantly involved in processes such as plasticity in the thalamocortical system (32).

We thank Steve Sollot, Terry Bunn, Rob Hampsen, Larry Andrews (NB Labs), and Harvey Wiggins (Spectrum Scientific) for technical support. This work was supported by Grants NS-26722, AFOSR-90-0266, and AA06965 to J.K.C., NS-29161 to R.C.S.L., and a fellowship from the Sao Paulo State Foundation for Research (88/4044-9) to M.A.L.N.

1. Mountcastle, V. B. & Henneman, E. (1952) *J. Comp. Neurol.* **97**, 409–439.
2. Powell, T. P. S. & Mountcastle, V. B. (1959) *Bull. Johns Hopkins Hosp.* **105**, 133–162.
3. Poggio, G. F. & Mountcastle, V. B. (1960) *Bull. Johns Hopkins Hosp.* **108**, 266–316.
4. Merzenich, M. M., Kaas, J. H., Wall, J. T., Nelson, R. J., Sur, M. & Felleman, D. J. (1983) *Neuroscience* **8**, 33–55.
5. Whitsel, B. L., Favorov, O., Tommerdahl, M., Diamond, M., Juliano, S. & Kelly, D. G. (1989) in *Sensory Processing in the Mammalian Brain*, ed. Lund, J. S. (Oxford Univ. Press, New York), pp. 84–116.
6. Jenkins, W. M., Merzenich, M. M., Ochs, M. T., Allard, T. & Guic-Robles, E. (1990) *J. Neurophysiol.* **63**, 82–104.
7. Chapin, J. K. (1987) in *Neural and Behavioral Approaches to Higher Brain Function*, eds. Wise, S. P. & Evarts, E. V. (Wiley, New York), pp. 181–209.
8. Waite, P. M. E. (1973) *J. Physiol. (London)* **228**, 527–540.
9. Rhoades, R. W., Belford, G. R. & Killackey, H. P. (1987) *J. Neurophysiol.* **57**, 1577–1600.
10. Chiaia, N. L., Rhoades, R. W., Fish, S. E. & Killackey, H. P. (1992) *J. Comp. Neurol.* **31**, 217–236.
11. Smith, R. L. (1973) *J. Comp. Neurol.* **148**, 423–446.
12. Peschanski, M., Mantyh, P. W. & Besson, J. M. (1983) *Brain Res.* **278**, 240–244.
13. Peschanski, M., Lee, C. L. & Ralston, H., III (1984) *Brain Res.* **297**, 63–74.
14. Erzurumlu, R. S., Bates, C. A. & Killackey, H. P. (1980) *Brain Res.* **198**, 427–433.
15. Chmielowska, J., Carvell, G. E. & Simons, D. J. (1989) *J. Comp. Neurol.* **285**, 325–338.
16. Minderhood, J. M. (1971) *Exp. Brain Res.* **12**, 435–446.
17. Simons, D. J. & Carvell, G. E. (1989) *J. Neurophysiol.* **61**, 311–330.
18. Armstrong-James, M. & Callahan, C. A. (1991) *J. Comp. Neurol.* **303**, 211–224.
19. Diamond, M. E., Armstrong-James, M. & Ebner, F. F. (1992) *J. Comp. Neurol.* **318**, 462–476.
20. Abeles, M. & Goldstein, M. (1977) *IEEE Proc.* **65**, 762–773.
21. Sarna, M. F., Gochin, P., Kaltenbach, J., Salganicoff, M. & Gerstein, G. L. (1988) *J. Neurosci. Methods* **25**, 189–196.
22. Chapin, J. K., Waterhouse, B. D. & Woodward, D. J. (1981) *Brain Res. Bull.* **6**, 63–70.
23. Chapin, J. K. & Lin, C. S. (1984) *J. Comp. Neurol.* **229**, 199–213.
24. Carvell, G. E. & Simons, D. J. (1990) *J. Neurosci.* **10**, 2638–2648.
25. Harris, R. M. (1986) *J. Comp. Neurol.* **251**, 491–505.
26. Williams, M. N., Zahm, D. S. & Jacquin, M. F. (1991) *Soc. Neurosci. Abstr.* **17**, 622.
27. Jacquin, M. F., Mooney, R. D. & Rhoades, R. W. (1986) *Exp. Brain Res.* **61**, 457–468.
28. Diamond, M. E., Armstrong-James, M., Budway, M. J. & Ebner, F. F. (1992) *J. Comp. Neurol.* **319**, 66–84.
29. Stevens, J. K. & Gerstein, G. L. (1976) *J. Neurophysiol.* **39**, 213–238.
30. Georgopolus, A. P., Swartz, A. B. & Ketter, R. E. (1986) *Science* **233**, 1416–1419.
31. Young, M. P. & Yamane, S. (1992) *Science* **256**, 1327–1331.
32. Nicolelis, M. A. L., Lin, R. C.-S. & Chapin, J. K. (1992) *Soc. Neurosci. Abstr.* **18**, 1392.